Proceedings of the 11th Brazilian Congress of Thermal Sciences and Engineering -- ENCIT 2006
Braz. Soc. of Mechanical Sciences and Engineering -- ABCM, Curitiba, Brazil,- Dec. 5-8, 2006

Paper CIT06-0647

NOZZLE SIZE EFFECT DURING LAMINAR COUNTERFLOW COMBUSTION

Antonio Pereira Roseira Junior
Seção de Mísseis e Foguetes / Divisão Bélica - Centro Tecnológico do Exército - 23020-470 - Rio de Janeiro - RJ - Brazil
aroseira@ctex.eb.br

Albino José Kalab Leiroz
Departmento de Engenharia Mecânica, POLI/ COPPE - Universidade Federal do Rio de Janeiro
Cx. Postal 68503 - Rio de Janeiro – RJ - 21945-970 - Brazil
leiroz@ufrj.br

Abstract. *This paper presents a numerical solution of a non-premixed methane-air flame in a modified two-dimensional counterflow geometry of slot burners. Solid walls are placed beside the burners as boundary conditions, providing a confined flow field. The development fields of flow, temperature and chemical species concentration are studied. A single-step chemistry mechanism is assumed to the reaction rate. The Finite-Difference Method is employed on the mass, momentum, energy and chemical species conservation equations, which are written in a Cartesian system of coordinates and discretized using the BTCS scheme. The Vorticity-Stream function formulation is used to solve the Navier-Stokes equations while the Shvab-Zel'dovich formulation solves the energy and chemical species ones. An iterative numerical technique based on successive under-relaxation and local errors control are computed to solve the resulting system of algebraic equations. A parametric study is conducted for different nozzle sizes, conjugated with variable inflow velocities of the reactants, and the results show the effects on the flame shape characteristics, subject to the presence of recirculation zones.*

Keywords *non-premixed flame, counterflow, vorticity-stream function, Shvab-Zel'dovich formulation.*

1. Introduction

The counterflow flame is commonly used for experimental combustion and chemical kinetic modeling studies of non-premixed combustion. When studying the interaction of heat and mass transfer with chemical reactions in commercial burners, gas turbines, and ramjets, these flames are important (Douglas, 1996). The counterflow configuration can be found in studies on the overall reaction rates for various fuel-oxidant combinations, the effectiveness of inhibitors (Tsuji, 1982), the transient phenomena during diffusion/edge flame transition (Frouzakis *et al.*, 2002) and the burning of multicomponent fuels in a diffusion flame (Fachini, 2001, 2004).

The interaction of a laminar vortex with a flame offers a scenario that is intermediate in complexity between laminar flames and turbulent ones. Furthermore, in a confined reacting counterflow, the vortex-flame interaction is also important. A significant recirculation zone can be produced due to the presence of a solid channel or duct walls (Roseira Jr and Leiroz, 2005). Since the steady-state counterflow diffusion flame represents well the local diffusion flame in unsteady distorted mixing layers in turbulent flow, studies on counterflow configuration can be taken to the flamelet model that is applied to non-premixed turbulent combustion (Peters, 1984).

Torikai *et al.* (1999) reported experimental studies to measure the blowoff limits of methane diffusion flames using a counterflow configuration, by closing a part of the fuel issuing exit with a solid disk set-up. In addiction, studies on interaction of laminar vortexes generated from either the fuel side or the oxidizer side (Santoro *et al.*, 1999), on flame-extinction phenomena (Pellet *et al.*, 1998, Daou and Liñán, 1999), and on the modeling of vortex-flame interactions (Amantini *et al.*, 2006) are also examples of the usage of the counterflow configuration.

In experiments, an inert co-flow curtain is often used to reduce the effects of air entrainment; as a result, the flame is confined only between the two nozzles. In numerical investigations, one-dimensional models along the axis of symmetry are almost exclusively used. Experimentally, Santoro *et al.* (2000) reported methane-air diffusion flames stabilized on an axisymmetric opposed jet burner with two parallel plates attached to the nozzle exists to confine the flow in the radial direction, and minimize entrainment while providing well-defined boundary conditions. The confinement induced to the flow field by adding solid walls beside the burners, provides a scenario where large recirculation zones can be generated, depending on the inflow conditions and on the relative size of the nozzle widths (Roseira Jr, 2005).

Although the analysis of such combustion events is a formidable task in real flow situations, or even in general laminar flows, it is instructive toward their understanding, to examine these events in simple prototypical flows. As an illustration of this approach, we shall analyze in this paper a combustion problem involving a non-premixed flame in modified two-dimensional counterflow geometry of slot burners is studied by a numerical approach. Adiabatic solid walls are placed beside the counterflow, creating a parallel flat plate channel. A parametric study is proposed to

investigate the influence of recirculation zones on the flame shape in the laminar regime, considering variations on the oxidizer inflow velocity and its nozzle width, in both coupled and uncoupled ways.

2. Physical and Mathematical Model

The physical model involves the combustion of two initially separate streams of fuel and oxidizer in gas-phase in a counterflow slot burner configuration. The configuration is commonly used in numerical and analytical studies since results are easily verified experimentally due to the easy access in the flame region (Fachini, 2001). The thermo-physical properties are assumed constant. In order to solve the Navier-Stokes equations, the Vorticity-Stream function formulation is employed, eliminating the pressure as a dependent variable from the momentum conservation equations and reducing the number of equations to be solved simultaneously. The continuity equation is identically satisfied by the stream function definition. The Vorticity-Stream function formulation presents a difficulty in the specification of vorticity boundary conditions. It is necessary to specify vorticity values along the solid boundaries in terms of the stream function, which requires the discretization using second order derivatives. Along the symmetry plane, zero-vorticity boundary condition is applied.

The description of diffusion flames imposing the Burke-Schumann kinetic model is relatively simple because there is no leakage of fuel and oxidizer through the flame. Consequently, the flow field can be specified by the gas properties without any information of the chemical reaction. Despite the simplicity of the mechanism, results obtained are still good to describe the problem with small leaking. Contrarily, flames near extinction or flames under high strain rate are incompatible with this model because the leaking of the reactants through the reaction zone is not negligible anymore.

The Simple Chemical Reaction System hypothesis is employed and the values of diffusivities of mass and energy are considered equal for each species. The mathematical model is based on the mass, momentum and mixture fraction conservation equations. The manipulation procedures done in the fluid dynamic and thermo-chemistry systems can be found in Anderson *et al.* (1984) and Kuo (1986).

The geometry adopted to represent the physical half-domain is described in a Cartesian system of coordinates by four boundaries, as illustrated by Fig. (1). The left boundary represents the flow field symmetry plane and the nozzles separation width (L^*), the right boundary is the outflow region, as well as the truncation position in the horizontal direction. The top and bottom boundaries (P^*) include the fuel and oxidizer nozzle widths, respectively, D_F^* and D_O^*, and the solid walls, which are considered adiabatic and nonreactive (Tomboulides *et al.*, 1997, Santoro *et al.*, 1999, Frouzakis *et al.*, 2002, Chaniotis *et al.*, 2003). This configuration offers the advantages of minimal heat losses, and nearly one-dimensional flame geometry in the vicinity of the stagnation plane (close to the symmetry plane). Traditionally, the non-premixed flame generated by this experimental configuration is analyzed in a one-dimensional context, whereas, in theoretical studies, the flow field near the stagnation plane is described by a simple potential stagnation flow solution.

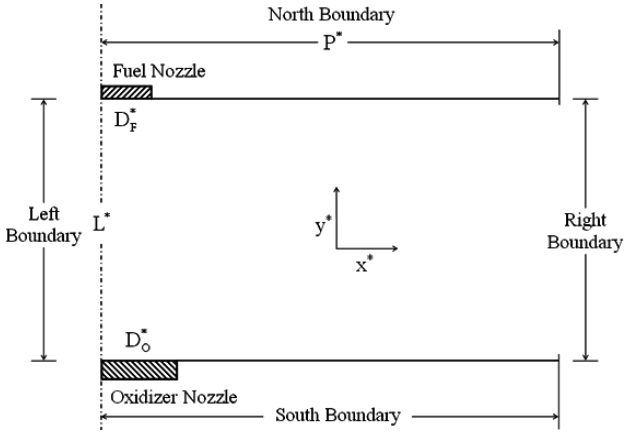

Figure 1. Geometry representing a half-domain.

The definitions of the dimensionless groups employed in the following equations are given by Eqs. 1.a-j.

$$x = \frac{x^*}{D_F^*} \quad ; \quad y = \frac{y^*}{D_F^*} \quad ; \quad L = \frac{L^*}{D_F^*} \quad ; \quad P = \frac{P^*}{D_F^*} \quad ; \quad u = \frac{u^*}{\left|U_F^*\right|} \quad ; \quad v = \frac{v^*}{\left|U_F^*\right|}$$

$$\xi = \frac{\xi^* D_F^*}{\left|U_F^*\right|} \quad ; \quad \psi = \frac{\psi^*}{\left|U_F^*\right| . D_F^*} \quad ; \quad t = \frac{t^* \left|U_F^*\right|}{D_F^*} \quad ; \quad \theta = \frac{T^* - T_F}{T_O - T_F} \qquad (1.a\text{-}j)$$

where U_F^* is the fuel peak velocity (at the top nozzle) and, T_F, T_O the respective fuel and oxidizer inflow temperatures.

The fluid dynamic system is described by the Navies-Stokes equations: mass and momentum conservation equations. However, by introducing the Vorticity-Stream function formulation, we can manipulate the momentum equations and use the definition of vorticity as

$$\xi = \frac{\partial v}{\partial x} - \frac{\partial u}{\partial y}, \tag{2}$$

which results in a Vorticity Transport equation

$$\frac{\partial \xi}{\partial t} + u\frac{\partial \xi}{\partial x} + v\frac{\partial \xi}{\partial y} = \frac{1}{Re}\left(\frac{\partial^2 \xi}{\partial x^2} + \frac{\partial^2 \xi}{\partial y^2}\right). \tag{3}$$

The Reynolds number is defined based on the fuel nozzle parameters

$$Re = \frac{\left|U_F^*\right|.D_F^*}{\upsilon} \quad ; \quad \upsilon \text{ is the fuel kinematic viscosity.} \tag{4}$$

Stream function $\psi(x,y)$ is defined, using the velocity components in order to satisfy the continuity equation, as

$$u = \frac{\partial \psi}{\partial y} \quad ; \quad v = -\frac{\partial \psi}{\partial x}. \tag{5.a-b}$$

Replacing the velocity components Eqs.(5.a-b) in Eq.(2), we obtain the Poisson's equation for the stream function

$$-\xi = \frac{\partial^2 \psi}{\partial x^2} + \frac{\partial^2 \psi}{\partial y^2} \tag{6}$$

Parabolic velocity profiles were used to represent the inflow velocity conditions at the nozzles and at the outflow boundaries. Therefore, the velocities boundary conditions must be expressed in terms of stream function, as

$$\begin{aligned}
&\psi = 0 \quad ; \quad x = 0 \ , \ 0 < y < \frac{1}{R_{DL}} \\
&\psi(x) = \frac{3x}{2}\left(1 - \frac{x^2}{3}\right) \quad ; \quad 0 \le x \le 1 \ , \ y = \frac{1}{R_{DL}} \\
&\psi = 1 \quad ; \quad 1 < x \le R_H \ , \ y = \frac{1}{R_{DL}} \\
&\psi(y) = y^2 R_{DL}{}^2 \left(1 + R_V.R_B\right)\left(3 - 2\,y\,R_{DL}\right) - R_V.R_B \quad ; \quad x = R_H \ , \ 0 < y < \frac{1}{R_{DL}} \\
&\psi(x) = -\frac{3x\,R_V}{2}\left[1 - \frac{1}{3}\left(\frac{x}{R_B}\right)^2\right] \quad ; \quad 0 \le x \le R_B \ , \ y = 0 \\
&\psi = -R_V.R_B \quad ; \quad R_B < x \le R_H \ , \ y = 0
\end{aligned} \tag{7.a-f}$$

The following dimensionless ratios represent, respectively, the fuel nozzle width-separation distance, the horizontal aspect, inflow peak velocities, and nozzle width ratios

$$R_{DL} = \frac{D_F^*}{L^*}, \quad R_H = \frac{P^*}{D_F^*}, \quad R_V = \frac{U_O^*}{\left|U_F^*\right|}, \quad R_B = \frac{D_O^*}{D_F^*} \tag{8}$$

The present study will be focused on the last two ratios, R_V and R_B.

The thermo-chemistry system is described by the energy and chemical species equations

$$\frac{\partial\theta}{\partial t}+u\frac{\partial\theta}{\partial x}+v\frac{\partial\theta}{\partial y}=\frac{1}{Pe}\left(\frac{\partial^2\theta}{\partial x^2}+\frac{\partial^2\theta}{\partial y^2}\right)+\frac{\dot{\omega}_F^*\,\Delta H_C}{\rho c_p(T_O-T_F)}\cdot\frac{D_F^*}{\left|U_F^*\right|} \tag{9}$$

$$\frac{\partial Y_i}{\partial t}+u\frac{\partial Y_i}{\partial x}+v\frac{\partial Y_i}{\partial y}=\frac{1}{Pe\,Le_i}\left(\frac{\partial^2 Y_i}{\partial x^2}+\frac{\partial^2 Y_i}{\partial y^2}\right)-\frac{D_F^*}{\left|U_F^*\right|}\frac{\dot{\omega}_i^*}{\rho} \tag{10.a-b}$$

Where $Pe=\dfrac{\rho\left|U_F^*\right|D_F^* c_p}{k}$, $Le_i=\dfrac{k}{\rho D_{ij} c_p}$, k is the thermal conductivity, ΔH_C is the heat release rate and $Y_i, \dot{\omega}_i^*$ are, respectively, the mass fraction in the mixture and consumption rate of the "i" specie. The mass diffusivity coefficients are considered equal for each species ($D_{ij}=D_{ji}=D$). The Simple Chemical Reaction System (SRCS) hypothesis is employed and the mixture fraction conservation equation can be obtained by following the assumption

$$1\text{ kg of Fuel} + s\text{ kg of Oxidizer} \longrightarrow (1+s)\text{ kg of Products} \tag{11}$$

For stoichiometric coefficients, n_F, n_o, and molecular weights of fuel and oxidizer, W_F, W_o, the mass-weighted stoichiometric coefficient ratio (s) can be written as

$$s=\frac{n_O.W_O}{n_F.W_F} \tag{12}$$

As consequence, the species consumption rates can be written as

$$\dot{\omega}_F^*=\frac{\dot{\omega}_O^*}{s} \tag{13}$$

Assuming $Le_F = Le_O = 1$ and manipulating the species equations (Eqs. 10.a-b), the first coupling variable and the correspondent conservation equation can be established as follows by

$$\phi_{FO}=Y_F-\frac{Y_O}{s} \tag{14}$$

$$\frac{\partial\phi_{FO}}{\partial t}+u\frac{\partial\phi_{FO}}{\partial x}+v\frac{\partial\phi_{FO}}{\partial y}=\frac{1}{Pe}\left(\frac{\partial^2\phi_{FO}}{\partial x^2}+\frac{\partial^2\phi_{FO}}{\partial y^2}\right) \tag{15}$$

In a similar way, the other two coupling variables and the dimensionless heat release rate (Q) can be expressed as

$$\phi_{TF}=Q.Y_F+\theta \quad ; \quad \phi_{TO}=\frac{Q.Y_O}{s}+\theta \quad \text{and} \quad Q=\frac{\Delta H_C}{c_p(T_O-T_F)}\ , \tag{16.a-c}$$

resulting in a linear relation among the coupling variables

$$\phi_{TO}=\phi_{TF}-Q.\phi_{FO} \tag{17}$$

The boundary condition for the fluid dynamics problem is the null velocity at solid boundaries, null tension at the left and right boundaries and prescribed parabolic velocities profiles at the inlet nozzles. For the heat and mass transfer problem, the boundary condition is the null diffusion flux along the solid walls and along the left and right boundaries. But at the fluid inlet, the mass fraction of the fuel is equal to one and the dimensionless temperature is zero at fuel nozzle, while at oxidizer nozzle the mass fraction is equal to one and the dimensionless temperature is equal to one. The initial condition is the stagnant, isothermal and inert medium.

3. Numerical Procedure

The Finite-Difference Method is employed on the resulting conservation equations, which are discretized using the BTCS (Backward in Time Centered in Space) scheme (Anderson *et al.*, 1984). An iterative numerical technique, based on the algorithm of the Gauss-Seidel with successive under-relaxation and local error control is applied to solve the resulting algebraic linear systems. A non-uniform structured mesh is employed with 121 x 41 points.

4. Results

Starting with a baseline case, two distinct analyses could be done. According with the formulation, Eq. 7-f represents the oxidizer inflow magnitude, in terms of stream function, where the velocity and nozzle-width ratios figure out. So, if we only modify the nozzle-width ratio, R_B, we'll be proportionally modifying the oxidizer inflow magnitude, which permits one sort of analysis. However, with objective to maintain the reactants inflow identical, in such a way that permits only the variation of the oxidizer nozzle width, the velocity ratio, R_V, must follow the inverse variation of the nozzle-width ratio, R_B, which permits a second analysis.

Therefore, the cases analyzed in the following subsections consider the variation of the R_V and R_B parameters, as illustrated by Tab. (1) below.

Table 1 – Cases analyzed with respect to the velocity ratio R_V and the nozzle-width ratio R_B.

	Re	**R_{DL}**	**R_H**	**R_V**	**R_B**
Case 1	50	0,5	6	1	1
Case 2	50	0,5	6	1	**0,5**
Case 3	50	0,5	6	**2**	**0,5**
Case 4	50	0,5	6	1	2
Case 5	50	0,5	6	**0,5**	2

4.1. Base Case analysis

The base case (Case 1) considers the following parameters: Reynolds number, Re = 50, R_{DL} = 0.5, R_H = 6, R_V = 1, R_B = 1, fuel nozzle length, D^*_F = 1, and distance between the nozzles, L^* = 2. The thermo-physical properties were chosen as Prandtl number, Pr = 0.7; ΔH_C = 802000 J/mol (Kuo, 1986); c_p = 30 J/mol.K; T_O = 400 K; T_F = 300 K; $Y_{O,in}$ = 0.233; $Y_{F,in}$ = 1.

The first conserved scalar can be normalized by the inflow condition, resulting in the following relation

$$\phi^*_{FO} = \frac{s.\phi_{FO} + Y_{O,in}}{s.Y_{F,in} + Y_{O,in}} \tag{18}$$

At the flame position ($\phi_{FO} = 0$) its stoichiometric value can be calculated as

$$\phi^*_{FO,St} = 0.05518 \tag{19}$$

The specific heat at constant pressure was considered constant at the average value between the air and the fuel at the nozzles temperatures (Fachini, 2004).

Figure (2) shows the results to the temperature field distribution. The black solid line represents the stoichiometric relation for the first conserved scalar (Eq. 14), and thus, where the combustion reaction takes place, indicating the flame position. Therefore, an underventilated flame can be observed, touching the bottom wall at the x = 3.8 coordinate. The flame is located next to the oxidizer nozzle (bottom) and also below the stagnation plane of the flow field (y = 1.0), as consequence of the identical reactants inflow magnitudes (R_V = 1). The displacement suffered by the stoichiometric line along the longitudinal direction is observed.

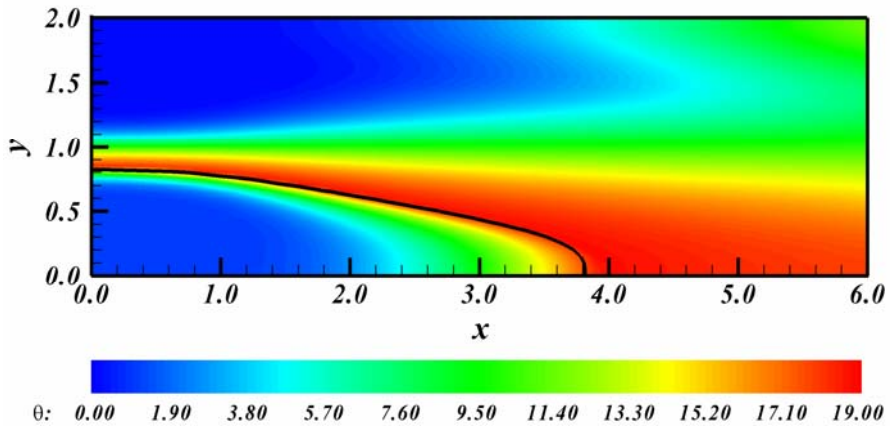

Figure 2. Temperature Field and Stoichiometric Line to the base case (Re = 50, R_{DL} = 0.5, R_H = 6, R_V = 1, R_B = 1)

The temperature field indicates the flame behavior and furnishes information about the hottest and coldest regions inside the counterflow channel. The hottest zone is linked with the flame position and the coldest one is observed faraway from the flame. Therefore, increasing the Reynolds number the flame reaches greater lengths of the channel. Then, increasing the Re the combustion chamber must be increased too.

4.2. Oxidizer Nozzle Reduction

Case 2 performs a reduction to the oxidizer nozzle width, which is also followed by its inflow magnitude. The Fig. (3) depicts a new flame behavior, where the stagnation plan of the flow field has moved away from the combustible nozzle. It can be easily observed that the stoichiometric line is now located practically in the neighborhood of the oxidizer nozzle, also compensating the lack of this specie to the chemical reaction.

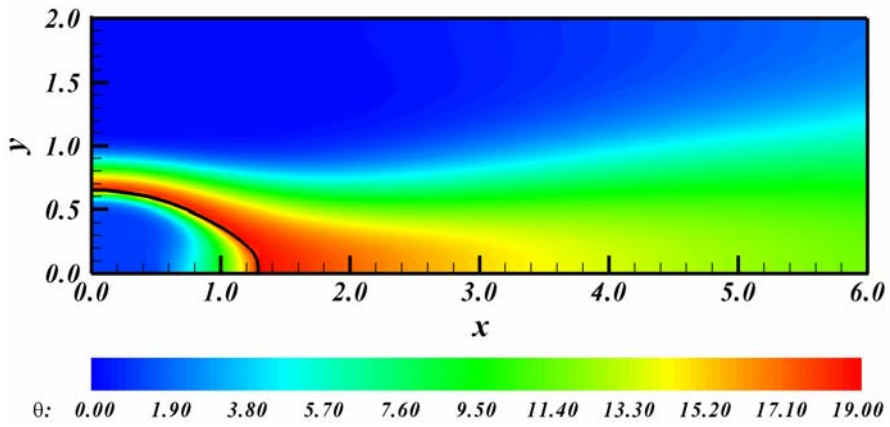

Figure 3. Temperature Field and Stoichiometric Line (Case 2 – Re = 50, R_{DL} = 0.5, R_H = 6, R_V = 1, R_B = 0.5)

Figure (4) illustrates the level curves of species mass fraction. The fuel level curves follow the preferential direction of the flow field, while the oxidizer curves are limited to the stoichiometric line position, remaining in the neighborhoods of the oxidizer nozzle. Since for a pure diffusion flame, the blowoff at the small reactant inflow velocity is due to thermal quenching by interaction between the flame and the nozzle surface, the flame observed in this case would possibly suffer a extinguish process for being anchored at the oxidizer nozzle, losing heat to it.

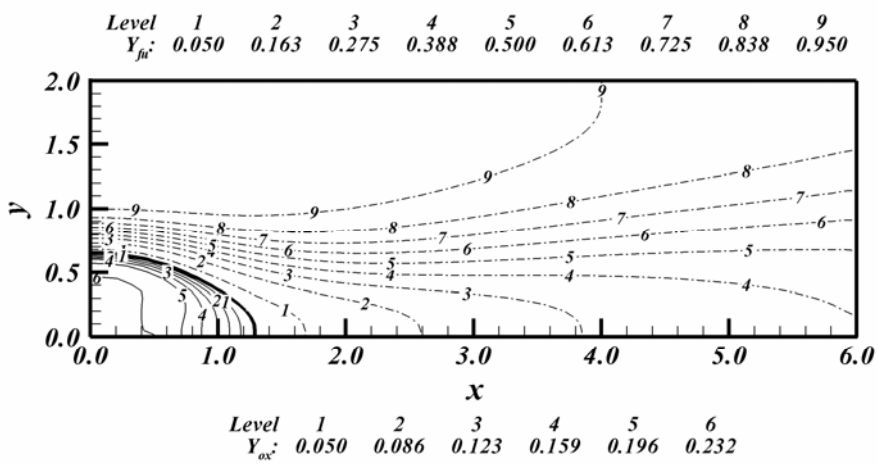

Figure 4. Mass Fraction curves of species (Case 2 – Re = 50, R_{DL} = 0.5, R_H = 6, R_V = 1, R_B = 0.5)

To illustrate more clearly the resulting aspects of the fields shown by Fig (4), the temperature and mass fraction profiles are plotted across the flame, which is along the axis of symmetry. Because the width of the oxidizer nozzle is a half of the combustible nozzle's (from x = 0 to x = 0.5), the transversal section for visualization of the respective profiles was chosen at x = 0.4, represented by Fig. (5).

This maximum value obtained to the dimensionless temperature field can only be achieved if the fuel and oxidizer are completely consumed during the reaction. It is known that the flame temperature of a non-premixed flame will always be equal to the adiabatic flame temperature of a premixed stoichiometric flame. With the adopted parameters, the calculated dimensionless adiabatic flame temperature was 15.7 (1869 K).

The overlap between fuel and oxidizer is infinitesimally small in the flame sheet model, but shown of finite width here, due to the number of points employed in the mesh.

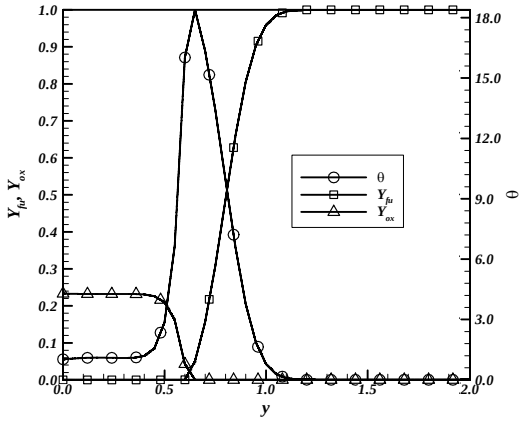

Figure 5. Temperature and Mass Fraction profiles at the transversal section x = 0.4 (Case 2)

In the following case (Case 3), the same reduction to the oxidizer nozzle width is performed again, however, its inflow magnitude is kept identical to the combustible one, by setting R_V = 2. The Fig. (6) shows the results for the temperature field and the stoichiometric line (solid line), where significant differences could be noted. Now, the stagnation plan of the flow field has moved towards the combustible nozzle, and the same behavior is observed to the stoichiometric line, which achieves a height of approximately y = 1.3, at the vertical symmetry plane. Also, a large recirculation zone (dash dotted lines) can be observed at the bottom wall, which consequently affects the level curves of the oxidizer mass fraction and the stoichiometric line itself, as shown by Fig. (7).

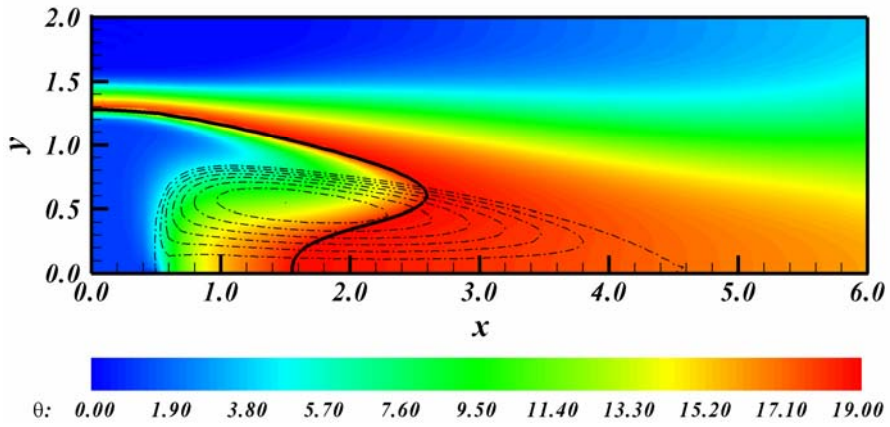

Figure 6. Temperature Field and Stoichiometric Line (Case 3 – Re = 50, R_{DL} = 0.5, R_H = 6, R_V = 2, R_B = 0.5)

The resulting interaction between the flame and the vortexes zones appears as a pronounced deformation of the flame shape in such area, as can be seen at x = 2.6. In other words, it indicates that the eddy zone holds the flame confined inside the counterflow channel. Depending on the Reynolds number range, changes on the nozzle widths can also serve as base to the sizing of the combustion chamber process, as well as to assist in the design and optimization of experiments.

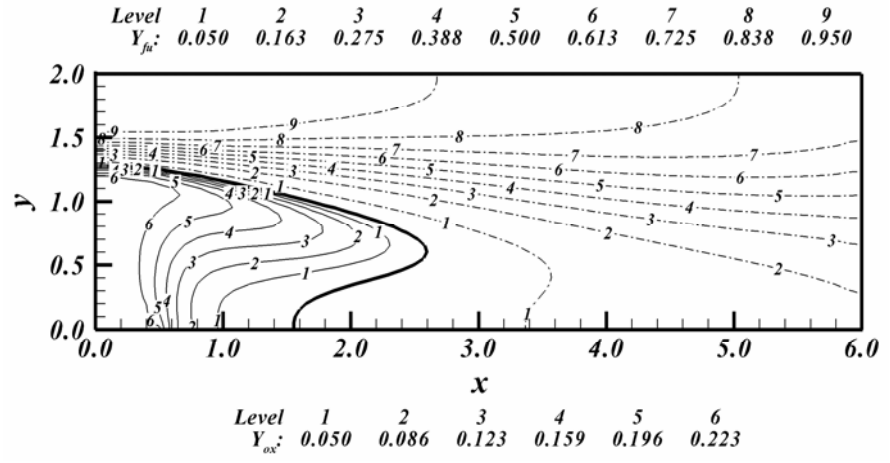

Figure 7. Mass Fraction curves of species (Case 3 – Re = 50, R_{DL} = 0.5, R_H = 6, R_V = 2, R_B = 0.5)

Figure (8) highlights the isolated effect of the oxidizer nozzle reduction, where, at the transversal section x = 0.4, the temperature profile indicates the position of the flame near to the combustible nozzle (top) and the presence of higher gradients to the temperature and mass fraction profiles. The effect of the recirculation zones to the temperature field is also noted, represented by non-monotonic behavior from y = 0 to y = 1. Inside this portion, it can be observed a value to the temperature profile higher than the inflow temperature at the oxidizer nozzle, at y = 0.

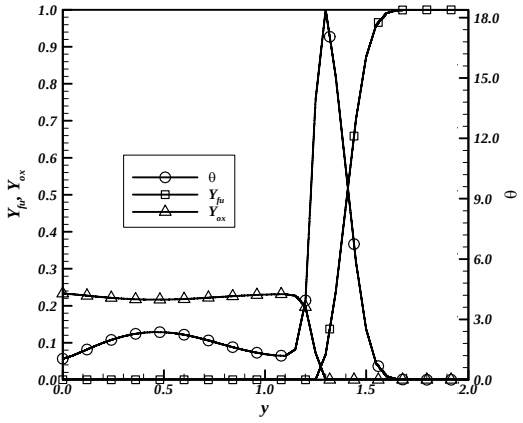

Figure 8. Temperature and Mass Fraction profiles at the transversal section x = 0.4 (Case 3)

4.3. Oxidizer Nozzle Increase

The two cases analyzed in this subsection consider an increase to the oxidizer nozzle width, by setting $R_B = 2$, however, in the Case 4, the oxidizer inflow magnitude is also increased, respectively. The Fig. (9) shows the stoichiometric line behavior, following the stagnation plan of the flow field. However, the flame presented here is not underventilated anymore, and the results show the flame crossing the exit boundary at x = 6. This result indicates the necessity to reevaluate the outflow boundary position to provide numerical solutions unaffected by the zero-Neumann outflow boundary conditions, which can be done by increasing the distance of the outflow boundary, moving it away from the symmetry plane as the flowrates are increased (Roseira Jr, 2005).

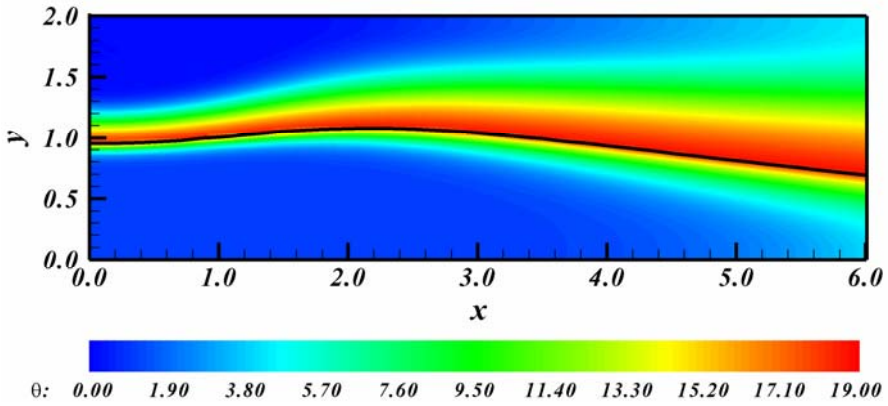

Figure 9. Temperature Field and Stoichiometric Line (Case 4 – Re = 50, $R_{DL} = 0.5$, $R_H = 6$, $R_V = 1$, $R_B = 2$)

Figure (10) depicts the level curves of the species mass fraction, which also follow the preferential direction of the flow field, due to convective process of transport. In addiction, there is no generation of recirculation zones because the oxidizer nozzle has a bigger width, from x = 0 to x = 2. Since the mean velocity of the oxidizer gases decreases, this results in a smooth inflow velocity profile, which tends to minimize the shear effects observed at the nozzle-wall interface region, responsible for the formation of eddies.

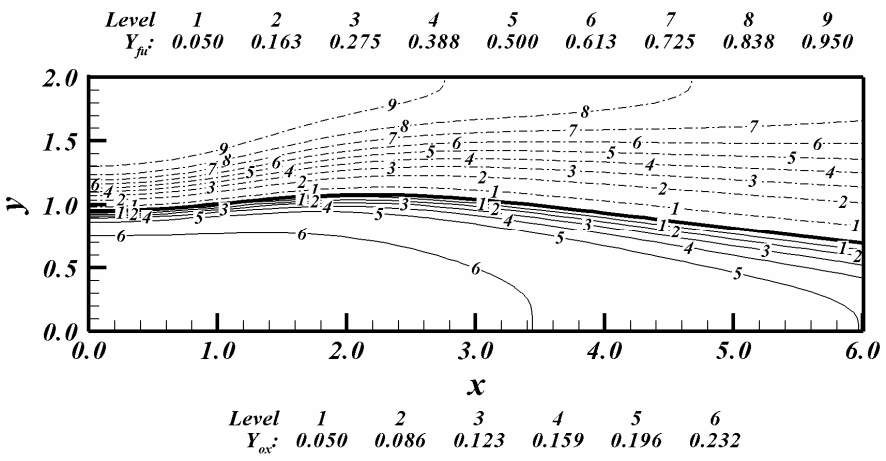

Figure 10. Mass Fraction curves of species (Case 4 – Re = 50, R_{DL} = 0.5, R_H = 6, R_V = 1, R_B = 2)

Therefore, the transversal section for visualization of the temperature and mass fraction profiles was chosen at *x = 1.6*, to maintain the proportional analogy with the former subsection, as illustrated below by Fig. (11).

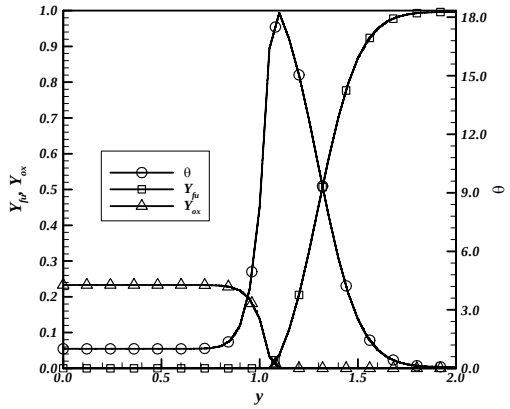

Figure 11. Temperature and Mass Fraction profiles at the transversal section x = 1.6 (Case 4)

Finally, in the Case 5, the oxidizer inflow magnitude is compensated by setting R_V = 0.5, which turns the reactants inflows identical again. As consequence, an underventilated flame can be observed again, as shown by Fig. (12). It can be noted that the stoichiometric line touches again the bottom wall at x = 4.2.

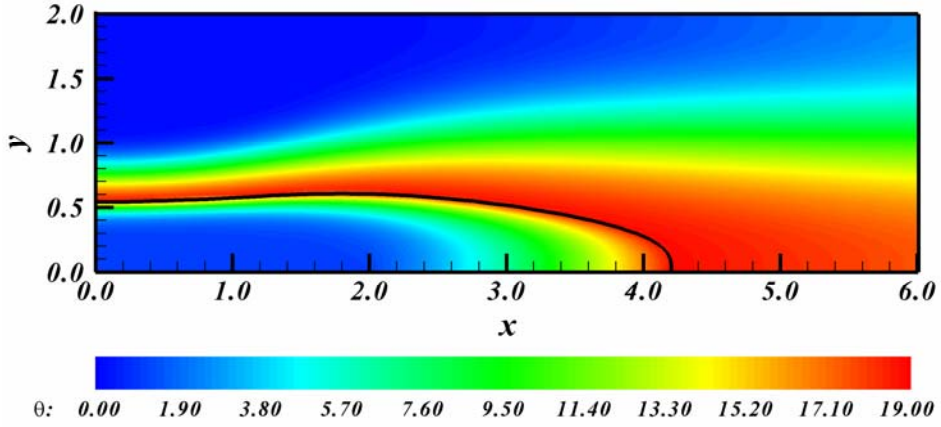

Figure 12. Temperature Field and Stoichiometric Line (Case 5 – Re = 50, R_{DL} = 0.5, R_H = 6, R_V = 0.5, R_B = 2)

Figure (13) depicts the combustible level curves of the mass fraction, which follow the preferential direction of the flow field, while the oxidizer levels are restrained by the stoichiometric line. Again, there is no generation of recirculation zones in this case due to the smooth inflow velocity profile at the oxidizer nozzle exit.

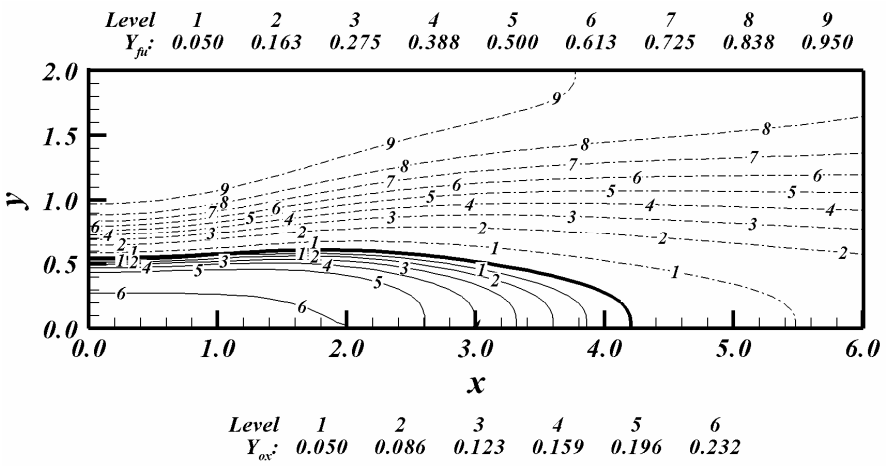

Figure 13. Mass Fraction curves of species (Case 5 – Re = 50, R_{DL} = 0.5, R_H = 6, R_V = 0.5, R_B = 2)

The temperature and mass fraction profiles illustrated by Fig 14 at the transversal section x = 1.6 indicate the expected approach of the flame to the oxidizer nozzle, however, the flame shown here is about three times longer than the flame of Case 2, but very similar to the flame of the base case, with respect to the longitudinal extension.

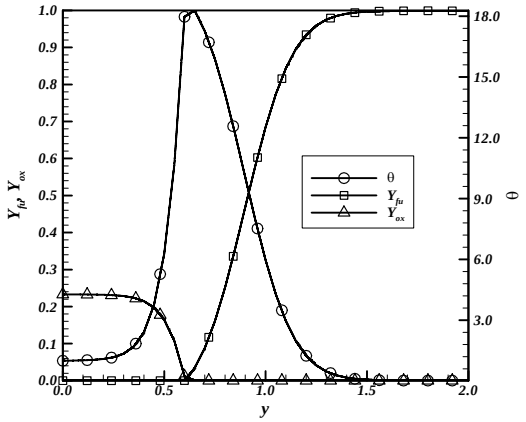

Figure 14. Temperature and Mass Fraction profiles at the transversal section x = 1.6 (Case 5)

5. Conclusions

In this work, we have described one possibility to control the position and shape of a non-premixed flame in a two-dimensional counterflow of reactive gases, in a parallel confined domain. Despite the one-step kinetics and simplified transport employed, the findings can be used to analyze the flame control event in the idealized flow under consideration, a step toward a better understanding of such events in realistic, more complicated flows.

The results have shown the existence of two distinct scenarios where an underventilated flame can be obtained and kept closer to a specific nozzle by varying the mass flowrate ratio and/or the inflow nozzle-width ratio of the opposing jets. Because of the two parallel walls used in the simulations, a large recirculation zone could be produced, as observed in the simulations of Tomboulides *et al.* (1997) and in the experimental work of Santoro *et al.* (2000).

Although recirculation zones are known to alter the stability of flames, that is an important field of research, since they can be used as a mechanism to maintain the flame held, as well as to improve the mixing effectiveness under laminar conditions in two-dimensional laminar confined opposing streams. It is relevant to note that such results will be certainly dependent of the Reynolds regime. Therefore, it is instructive to examine the range of flowrates, and complementary aspects between the present results and the closely related recent findings, since this point was not investigated in the present study.

Future work will investigate the combined simulation of detailed chemical kinetics and transport modeling to study the effect of fuel composition, inlet temperature and geometry, in order to determine more efficiently another critical parameters, taking into account compressibility effects due to heat release in the flame zone.

6. References

Amantini, G., Frank, J. H., Smooke, *et al.*, 2006, "Computational and Experimental study of Steady Two-dimensional Axisymmetric Non-Premixed Methane Counterflow Flames", to appear in Combustion Theory and Modeling.

Anderson, D. A., *et al.*, 1984, "Computational Fluid Mechanics and Heat Transfer", New York: Hemisphere Publishing Corporation.

Chaniotis, A. K., Frouzakis, C. E., Lee, J. C., *et al.*, 2003, "Remeshed smoothed particle hydrodynamics for the simulation of laminar chemically reactive flows", Journal of Computational Physics, Vol. 191, No.1, pp. 1-17.

Daou, J. and Liñán, A., 1999, "Ignition and extinction fronts in counterflowing premixed reactive gases", Combustion and Flame Vol. 118, pp. 479-488.

Fachini, F. F., 2001, "N-Fuels Diffusion Flame: Counterflow Configuration", Proceedings of XVI Congresso Brasileiro de Engenharia Mecânica, CD ROM, Uberlândia, MG, Brazil.

Fachini, F. F., 2004, Multicomponent Fuel Diffusion Flames: A General Shvab-Zel'dovich Formulation, "under consideration for publication".

Frouzakis, C. E., Lee, J. C., Tomboulides, D., *et al.*, 2002, "From diffusion to premixed flames in an H_2-Air opposed-jet burner: the role of edge flames", Combustion and Flame, Vol. 130, pp.171-184.

Kuo, K. K., 1986, "Principles of Combustion", USA, Wiley-Interscience.

Pellett, G. L., Isaac, K. M., Humphreys, W. M., *et al.*, 1998, "Velocity and Thermal Structure, and Strain- Induced Extinction of 14 to 100% Hydrogen-Air Counterflow Diffusion Flames", Combustion and Flame, Vol. 112, No. 4, pp. 575-592.

Peters, N., 1984, "Laminar Diffusion Flamelet Models in Non-premixed Turbulent Combustion", Prog. Energy Combust. Sci., Vol. 10, pp. 319-339.

Roseira Jr, A. P. and Leiroz, A. J. K., 2005, "A Parametric Study of a Confined Stagnation Methane-Air Diffusion Flame", Proceedings of 18th International Congress of Mechanical Engineering, CD ROM, Ouro Preto, MG, Brazil.

Roseira Jr, A. P., 2005, "Numerical Study of Laminar Confined Counterflows", M.Sc. Dissertation, Departmento de Engenharia Mecânica, COPPE, Universidade Federal do Rio de Janeiro, Rio de Janeiro, RJ, Brazil.

Santoro, V.S., Kyritsis, D. C., Gomez, A., 1999, "Extinction Behavior of either Gaseous or Spray Counterflow Diffusion Flames Interacting with a Laminar Toroidal Vortex", 17th International Colloquium on the Dynamics of Explosions and Reactive Systems, Heidelberg, Germany.

Santoro, V. S., Liñán, A., Gomez, A., 2000, "Propagation of edge flames in counterflow mixing layers: experiments and theory", Proc. Combust. Inst., Vol. 28, pp. 2039-2046.

Tomboulides, A. G., Lee, J. C., Orszag, S. A., 1997, "Numerical Simulation of Low Mach Number Reactive Flows", Journal of Scientific Computing, Vol. 12, No. 2, pp. 139-167.

Torikai, H., Matsuo, A., Ueda, T., *et al.*, 1999, "Characteristics of the Diffusion Flame with a Hole in the Stagnation Region of an Axisymmetric Impinging Jet", 17th International Colloquium on the Dynamics of Explosions and Reactive Systems, Heiderberg, Germany.

Tsuji, H., 1982, "Counterflow Diffusion Flames", Progress Energy Combustion Science, Vol.8, pp. 93-119.